September 25, 2025

Re: Simpson Strong-Tie® MPSC™ Mass Timber Point-Supported Column Connection – Seismic Deformation Compatibility Assessment

To Whom It May Concern:

Simpson Strong-Tie has evaluated the MPSC Mass Timber Point-Supported Column connection for seismic deformation compatibility. MPSC connection (Figure 1) connects top and bottom timber columns and supports mass timber floor panels to transfer vertical download. This engineering letter presents a simple analytical method to check whether the rotation is provided by the steel or the screw connection, and a finite element (FE) analysis to validate the seismic deformation capability up to 5% inter-story drift of the MPSC and the corresponding lateral load applying to the connection at this drift level less than the ASD lateral capacity of the connection.

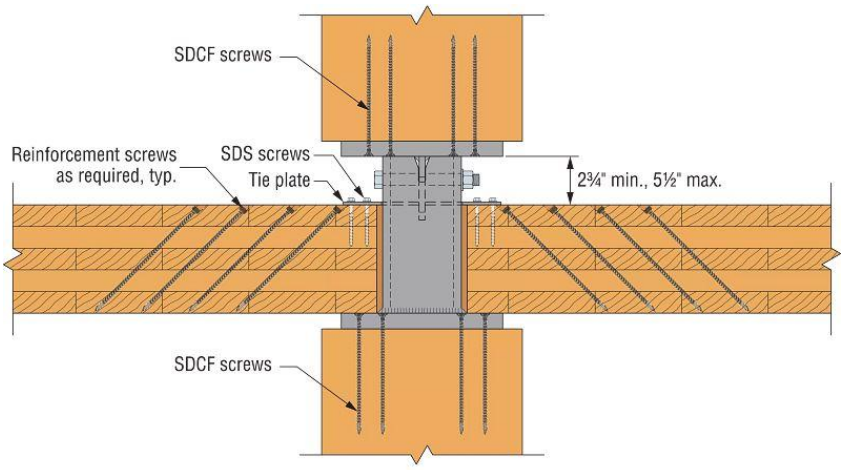

***Figure 1**: Overview of MPSC Connection*

Input and Material Models

The timber column was assumed to be 9-ft long, Douglas-Fir glulam with $f_{c,0}$ = 2400 psi and E_{col} = 2000 ksi. An elasto-plastic model was utilized to simulate the mechanical behavior of the timber column (Fig. 2). The model helps to refine the timber stress distribution at the bottom end of the column, which is crucial to predict the withdrawal of the screw connection. To develop the elasto-plastic model for DF glulam, the characteristic value of ultimate strength (f_{uw}) was determined as 1.9×f_{co} (4560 psi), 1.9 being the adjustment factor for compressive strength parallel to grain (ASTM D5456-19). The yield strength (f_{yw}) was assumed to be 60% of the ultimate strength, which is similar to the approach used in several previous studies (Sinha et al. 2024, Wei et al. 2019). A nonlinear spring model was applied to model the screw connection. A phenomenological model is used to describe the behavior of SDCF10x200 screw connection between the top part and the wood column in the FEA model. The combined withdrawal and lateral shear connection behavior is based on the physical test data of a single SDCF screw connection.

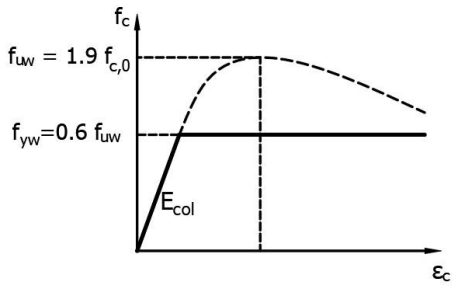

Figure 2: *Timber Material Model*

Analytical Method

The drift (or lateral displacement) at the top of a column, comprised of the flexural deflection of the column and the displacement due to rotation (or rocking) at the column base, is caused by the combination effect of vertical download and bending moment. The shear deformation is small and ignored in the analysis. There are two possible sources of the column base rotation depending on the loading condition. In Case 1, the rotation comes from the steel connection through the uplift of the top part from the bottom part of MPSC. In Case 2, the rotation is initiated when the column uplifts from the top bearing plate due to the screw withdrawal at the interface of timber column – to – top bearing plate. The analytical method presented in the following sections is utilized to evaluate the conditions for the onset of these two uplift cases and determine which case governs the uplift behavior. The effect of the notch cut at the top end of HSS is ignored to simplify the analysis; therefore, the uplift behavior of the connection in two major axes is identical.

Uplift Between Top and Bottom Parts of MPSC (Case 1)

The vertical download, P, and the flexural moment, M, are transferred from the top bearing plate to the HSS standoff and results in a distributed compressive stress at the top end of HSS as shown in Figure 3a. When the flexural moment is large enough, there will be a point on the top end of the HSS where the stress reaches zero and the uplift of the top bearing plate over the HSS will start happening. The top bearing plate will pivot around the compression area at the top end of the HSS. The HSS material at the top end is assumed to be still in the elastic range at the onset of the uplift.

The following equation shows the condition at the onset of the uplift.

$$\frac{P}{A_{HSS}} - \frac{F_{x,1}L_{col}}{S_{HSS}} = 0 \qquad \text{(Eq.1)}$$

In which:

A_{HSS} = Cross-section area of HSS.
S_{HSS} = First moment of area of HSS about the axis perpendicular to the direction of lateral load.
$F_{(x,1)}$ = Lateral load applied at the top of the column, causing the onset of uplift between the top and bottom parts of MPSC
L_{col} = Length of the wood column

Uplift of Column Base Due to Screw Withdrawal (Case 2)

Considering the equilibrium condition of the column, vertical download and lateral load will cause a distributed stress in the compression area at the bottom end of the column limited by the bearing area provided by the top plate. The onset of column uplift is assumed when the compressive stress at the location of the outermost screw reaches zero, which means the length of the compression area (c) equals the distance from the outermost screw to the corner (point O) of the column (L_s).

The distribution of compressive stress at the bottom of the column is assumed to be linear (when the wood material is still in elastic range) or trapezoid shape (for elasto-plastic model when the wood material exceeds the elastic range) as shown in Figure 3b.

The maximum compressive stress (f_{cmax}) is given by (Eq.2)

$$f_{cmax} = \frac{2P}{L_s \times t} \qquad \text{(Eq.2)}$$

In which: t and b = the dimensions of top bearing plate perpendicular and parallel to the lateral loading direction, respectively.

If f_{cmax} is less than the yield compressive strength of the column material (f_{yw}), the wood material is in elastic range. The lateral force causing the onset of column uplift (Case 2), $F_{x,2}$, is determined from the moment equilibrium equation and is given as:

$$F_{x,2} = \frac{P}{L_{col}} \times \left(\frac{b}{2} - \frac{L_s}{3}\right) \qquad \text{(Eq.3)}$$

If f_{cmax} obtained by Eq.2 is equal to or greater than f_{yw}, the crushing of timber material at the bottom of the column occurs. The elasto-plastic material model is utilized and f_{cmax} equals to f_{yw}. the length of the plastic area, c_p, and $F_{x,2}$ are determined by the following equations:

$$c_p = \frac{2P}{f_{yw} \times t} - L_s \qquad \text{(Eq.4)}$$

$$F_{x,2} = \frac{1}{L_{col}} \times \left[\frac{P \times b}{2} - \frac{f_{yw} \times t}{6}\left(L_s^2 + L_s c_p + c_p^2\right)\right] \qquad \text{(Eq.5)}$$

After calculating $F_{x,1}$ and $F_{x,2}$, the smaller of these two values with its corresponding uplift case will govern the rotation mechanism at the bottom of the column.

The analytical method was used for analysis of all five MPSC SKUs at different vertical load levels up to their download capacity. Since the stress distribution at the bottom of the timber column is considered within the bearing area provided by the top plate, the timber cross section used for the analysis of each MPSC SKUs is the same as the size of the corresponding top bearing plate.

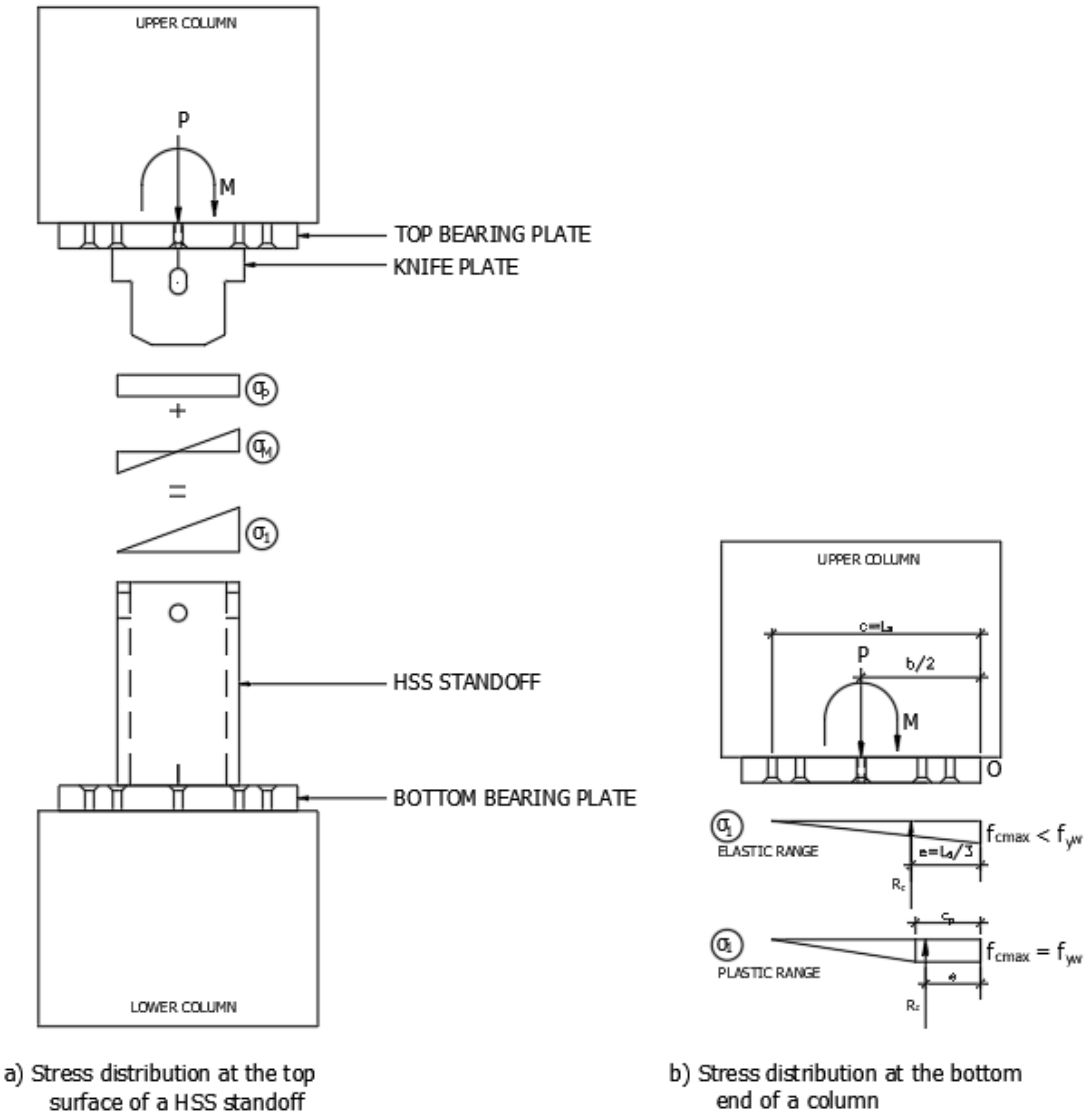

a) Stress distribution at the top surface of a HSS standoff

b) Stress distribution at the bottom end of a column

Figure 3: *Stress Distributions for Analytical Method*

Finite Element Analysis (FEA)

The simple analytical method for hand calculation presented above is utilized to determine when and where the rotation at the column base will occur first. However, to evaluate the connection performance after the onset of the column base rotation and up to 5% drift level, the analytical method becomes more complicated. In addition, the analytical method is simplified by considering the screw connection and steel connection working independently. To achieve a more accurate evaluation of the system drift performance, FEA was implemented to evaluate whether the drift capability of the column connection would be provided by the steel connection between the top and bottom parts of the MPSC (Case 1) or the screw connection between the top bearing plate and the upper column through the withdrawal behavior of screws (Case 2).

A Finite Element (FE) model was developed in ABAQUS to simulate the behavior of the connection under a combination effect of lateral load and vertical download. Since the geometry of the notch and the bolt connection is similar among different MPSC SKUs, MPSC300 is selected to represent MPSC connection in FEA. The model comprised an MPSC300 connection and a 15in. x 15in. upper glulam column. The bottom surface of the bottom bearing plate was modelled in fixed conditions. The top bearing plate was connected to the column by 12 SDCF10x200 screws that are required for the MPSC300 connection (Figure 4).

Six different cases of vertical download (50-kip, 100-kip, 150-kip, 200-kip, 250-kip and 300-kip) were considered. The vertical download was applied at the center of top end of the column as the "zero" state of the FE model to simulate the gravity load the column and MPSC300 connection would carry in a building. Then, the column was laterally pushed incrementally at the top end to 5% drift. Three different lateral drift directions, including perpendicular, parallel and 45-degree to bolt axis, were considered to evaluate the drift performance of the connection in different directions.

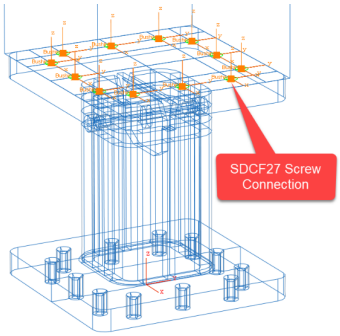

Figure 4: *Screw elements in FEA model*

Results and Discussion

The analytical results show that the column drift comes from rotation of the steel connection (Case 1) in most loading cases. The only exceptions are for MPSC250 and MPSC300 at their maximum download, at which the rotation from the screw connection (Case 2) was observed. Table 1 presents the results for MPSC300 at different vertical load levels.

Table 1: *Analytical Results*

SKU	Ls (in)	P (kip)	Fx,1(lbf)	cp (in)	Fx,2 (lbf)	Uplift Case
MPSC300	10.25	50	*728*	0	1144	Case 1
		100	*1456*	0	2282	Case 1
		150	*2184*	0	3420	Case 1
		200	*2912*	2.21	4316	Case 1
		250	*3640*	5.32	4293	Case 1
		300	4368	8.43	*3309*	*Case 2*

To observe the uplift from FEA result, the vertical displacements at screw locations (Figure 4), and at points on the bearing interface of the steel connection (Figure 5) were captured. In addition, the lateral force at the top end and withdrawal forces of all screws were recorded.

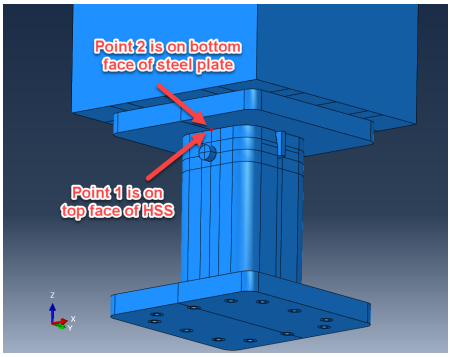

Figure 5: *Points on Steel Connection for Observing Uplift Behavior When Loading Parallel to Bolt Axis*

The FEA results presented in Table 2 show that the column base rotation for MPSC300 at all load levels are primarily from the steel connection. For vertical load levels from 50 to 200 kips, the hand calculation of analytical model underestimated the lateral load at the onset of uplift by less than 8.6%. However, at 250-kip and 300-kip download, the FEA results show considerably lower lateral loads at the onset of uplift than those calculated from the analytical method because the HSS was assumed to be in elastic range in the analytical method while the yielding was observed at certain areas in the HSS from FEA. At 5% drift, there was a very small rotational contribution from screw connection, indicated by small maximum withdrawal load in screws of less than 400 lbs. (as shown in Table 2) which are much lower than the ASD end grain withdrawal capacity of approximately 1200 lbs. per screw. The lateral load increases with the increase of the download, which causes more flexural deflection, and therefore, the steel connection rotation reduces. In all cases, the lateral load at 5% drift is less than the ASD lateral capacity of the MPSC300 (6.545 kip). The result confirms that the MPSC connection can accommodate a lateral drift of 5% (Figure 6).

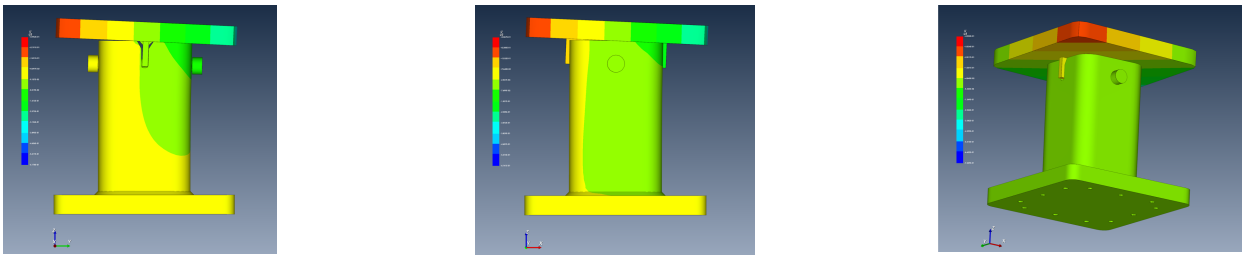

a) *b)* *c)*

Figure 6: *Steel Connection Rotation and Vertical Displacement of MPSC300 at 5% Column Drift: a) Loading Parallel to Bolt Axis, b) Loading Perpendicular to Bolt Axis, and c) Loading 45 degrees to bolt axis.*

Table 2: *FEA results for MPSC300*

Loading Direction	Vertical load (kip)	Lateral load @ uplift onset (kip)	@ 5% drift				Uplift Case
			Lateral load (kip)	Plate uplift (in)	Max. Screw Withdrawal Force (kip)	Steel Connection Rotation	
Parallel	50	0.754	1.442	0.268	0.081	4.81%	Case 1
	100	1.593	2.704	0.248	0.075	4.74%	Case 1
	150	2.379	3.883	0.222	0.089	4.66%	Case 1
	200	3.172	4.950	0.183	0.100	4.58%	Case 1
	250	3.321	5.795	0.142	0.124	4.50%	Case 1
	300	2.375	6.214	0.087	0.136	4.43%	Case 1
Perpendicular	50	0.751	1.852	0.231	0.374	4.67%	Case 1
	100	1.481	3.089	0.215	0.271	4.64%	Case 1
	150	2.373	4.224	0.215	0.222	4.59%	Case 1
	200	3.012	5.157	0.182	0.157	4.56%	Case 1
	250	3.328	5.957	0.145	0.144	4.51%	Case 1
	300	2.250	6.454	0.096	0.136	4.45%	Case 1
45 deg.	50		1.589	0.289	0.048	4.81%	Case 1
	100		2.946	0.250	0.072	4.72%	Case 1
	150		4.058	0.222	0.090	4.63%	Case 1
	200		4.934	0.188	0.102	4.60%	Case 1
	250		5.645	0.174	0.120	4.55%	Case 1
	300		6.095	0.138	0.139	4.50%	Case 1

The information in this letter is valid until **12/31/2026** when it will be re-evaluated by Simpson Strong-Tie. Please visit strongtie.com for additional pertinent information. If you have questions or need further assistance regarding this matter, please contact the Simpson Strong-Tie Engineering Department at 800-999-5099.

Sincerely,

SIMPSON STRONG-TIE COMPANY INC.

References

ASTM (2015). "ASTM A1085-15: Standard specification for Cold-Formed Welded Carbon Steel Hollow Structural Section (HSS)", American Society for Testing and Materials, 100 Barr Harbor Drive, PO Box C700, West Conshohocken, PA, 19428-2959 USA.

ASTM (2019). "ASTM D5456-19: Standard Specification for Evaluation of Structural Composite Lumber Products", American Society for Testing and Materials, 100 Barr Harbor Drive, PO Box C700, West Conshohocken, PA, 19428-2959 USA.

Sinha, A., Barbosa, A.R., Ho, T.X., Zimmerman, R.B., and McDonnell, E. (2024). "Compression behavior of cross-laminated timber wall panels with different reinforcement mechanisms", Journal of Materials in Civil Engineering, 2024, 36(8):04024223.

Wei, P., Wang, B.J., Li, H., Wang, L., Peng, S., and Zhang, L. (2019). "A comparative study of compression behaviors of cross-laminated timber and glued-laminated timber columns", Construction and Building Materials, 222(2019) 86-95.